ISSN 2176-5480

22nd International Congress of Mechanical Engineering (COBEM 2013)
November 3-7, 2013, Ribeirão Preto, SP, Brazil

FATIGUE CRACK GROWTH BEHAVIOR OF LASER BEAM AND FLASH WELDED JOINTS IN A MICROALLOYED HSLA STEEL

Henrique Varella Ribeiro
Carlos Antonio Reis Pereira Baptista
EEL/USP - Escola de Engenharia de Lorena da Universidade de São Paulo
Campus II, Polo Urbo-Industrial, Gleba AI-6, Lorena-SP, Brazil
henriquevarella@usp.br
baptista@eel.usp.br

Milton Sergio Fernandes de Lima
IEAv/DCTA – Instituto de Estudos Avançados
Rodovia dos Tamoios, São José dos Campos-SP, Brazil
msflima@yahoo.com.br

Marcelo Augusto Santos Torres
FEG/UNESP – Universidade Estadual Paulista "Júlio de Mesquita Filho"
Av. Ariberto Pereira da Cunha, 333, Guaratinguetá-SP, Brazil
mastorres@uol.com.br

Abstract. *The present study aims to evaluate the microstructure and fatigue crack growth (FCG) behavior of flash-welded and laser beam (LBW) joints of a 0.08%C-1,5%Mn (wt. pct.) microalloyed steel, recently developed by a Brazilian steel maker under the designation B550. This steel is being considered to stand in for the current SAE 1010 low carbon steel in wheel rims for trucks and busses. The flash welding process is currently used in the production of wheel rims. On the other hand, the lower heat input applied by LBW favors the austenite nucleation and thus the refining of the final grain size in the weld fillet. The microstructural evaluation was performed at the base metal, heat affected zone (HAZ) and weld metal. Compact Tension C(T) specimens were chosen for the fatigue tests. The loading was sinusoidal with constant amplitude, frequency of 10 Hz and stress ratio R = 0.1. The fatigue crack growth rate in the Paris regime of the welded region and HAZ was assessed and compared to that of the base material. The obtained results provide support for the understanding on how these welding processes and the welding parameters affect the materials properties and allowed correlating the mechanical strength and crack growth rate with the microestrutural characteristics. It was observed that the heat input is a major factor affecting the final characteristics of the joint. Among the obtained joints, one of the adopted LBW conditions presented the best FCG resistance.*

Keywords: *Microalloyed Steels, Flash Welding, Laser Beam Welding and Fatigue Crack Growth.*

1. INTRODUCTION

The need for reduction of the vehicles' weight led to the development of steels with improved chemical composition and microstructure. The high strength and low alloy (HSLA) steels have been considered as promising alternatives to the conventional carbon steels for the production of automotive parts such as chassis components, suspension arms and wheels. Their appeals are the high yield and ultimate strengths, chemical resistance, weldability and formability. These steels have low or medium carbon content and small additions of alloy elements such as Mn, Nb, Mo, V and Ti. These alloying elements are added mainly to control the austenitic grain size, to retard the austenite recrystallization and to promote precipitation hardening. The flash welding process is currently used in the production of low carbon steel wheel rims. Flash welding is a low-cost and high-efficiency welding method; in this welding technique, the parts to be joined are pressed against each other by means of non-consumable electrodes, between which an electrical current is established (Saito and Ichiyama, 1996). The contact occurs at discrete points, by which the electric current is established, causing the flash. The thermal potential is proportional to time, electric resistance and current intensity and should be enough to fully melt the metal in the contact region (Kang and Min, 2000). During the flash welding process, due to the absence of a protective gas, some discontinuities coming from impurities may form in the weld bead. If the flash energy is adequately controlled, the oxide impurities may be expelled together with the metal particles ejected in the flash. At the end of the process, when the compressive load is applied, the majority of the remaining impurities are removed as burr with the plastically deformed material (Ichiyama and Kodama, 2007). Low intensity electrical current and insufficient compressive load are the major causes of porosity and inclusions in the weld metal. Besides, the complex microstructures presented in the welded region may cause problems, such as joint embrittlement. During many years, car wheel rims have been assembled via flash welding, a method which fulfilled the demand of automobile

ISSN 2176-5480

manufacturers for high process speed and high volume scenario. But due to changes in the scenario, other welding methods are also gaining popularity in the industry (Fabari et al., 2010), like laser beam welding (LBW). The laser beam welding of HSLA steels is of considerable interest as it permits the obtaining of joints with low overall heat input, low distortion, high welding speeds, small heat affected zones, deep penetration, the potential for automation and the inherent flexibility of the laser system (Lin Li et al., 2011; Onõro and Ranninger, 1997). In this process, when an intense laser beam is focused on the workpiece, the material under the beam evaporates and generates a cavity, called keyhole. What maintains the keyhole is the equilibrium between the vapor pressure, which acts to open it, and the metalostatic pressure, which tends to close it. This equilibrium depends on the speed and power of the laser beam, among other parameters. For a fixed power, excessive speeds cause the collapse of the keyhole and low speeds result in a high material loss due to vaporization, as well as pore generation (Meie t al., 2009; Yi et al., 2008). The laser process is conducted without metal addition and needs a protective gas for the optics (normally nitrogen) and also a protection atmosphere for the weld bead, usually inert gases such as argon and helium. The latter is recommended for steel welding, because it decreases the formation of plasma, which absorbs and disperses the laser beam (Chung et al., 1999). In applications such as wheel production, welding and joining have to be involved, which would lead to localized material modifications and create potential safety and reliability issues under cyclic loading (Fabari et al., 2010), so that the characterization of fatigue crack growth of the welded joints is necessary.

The present study aims to evaluate the microstructure, tensile properties, microhardness profile and fatigue crack growth behavior of flash-welded and LBW joints of a 0.08%C-1,5%Mn (wt. pct.) microalloyed steel, recently developed by a Brazilian steel maker under designation B550. This steel is being considered to stand for the current SAE 1010 low carbon steel in wheel rims for trucks and busses. The microstructural evaluation was performed at the base metal, heat affected zone and weld metal, using optical microscopy. Compact Tension C(T) specimens were chosen for the fatigue tests. The loading was sinusoidal with constant amplitude, frequency of 10 Hz and stress ratio R = 0.1. The fatigue crack growth rate in the Paris regime of the welded region was assessed for both welding processes and compared to that of the base material. Scanning electron microscope (SEM) analyzed the samples fractured surfaces. Two low heat input and one high heat input welding processes were studied: fiber laser welding under two conditions of heat input and flash welding. The obtained results provide support for the understanding on how these welding processes affect the materials' properties and allowed correlating the mechanical strength and crack growth rate with the microestrutural characteristics.

2. EXPERIMENTAL PROCEDURE

2.1 Material and welding processes

The chemical composition of the B550 steel, recently developed by Companhia Siderúrgica Nacional (CSN) is given in Tab. 1. The butt joints made of 5 mm thick plates were produced by the flash welding process and laser beam welding. Flash welding was conducted in the wheels production line at IOCHPE-MAXION, using a HESS WO 4158 machine, and the welding parameters were determined in order to result in a continuous weld bead, as shown in the macrography of Fig. 1(a), and the material's flow line is given by Fig. 1(b). The laser beam welding was performed at the Instituto de Estudos Avançados (IEAv), using the high power fibre laser from IPG Photonics, model YLR-2000. Fiber laser was selected for welding experiments because of its good beam quality and high absorption factor. The employed laser has maximum power of 2 kW, operates in the continuum mode with beam quality of $M^2 \approx 12$. The welding parameters for the two adopted conditions were: maximum beam power (2 kW), helium protection with an outflow of 30 l/min at the melting region, focus on the surface and beam normal to the workpiece. The varied parameters were the welding speed and the number of passes, resulting in two welding conditions, referred as Laser-A and Laser-B. With Laser-A condition, the steel pieces were joined with a speed of 50 mm/s and two welding passes, one of them in the face and the other in the weld root, as shown inf Fig. 1(c) and 1(d). With Laser-B condition, the welding speed was 8 mm/s and only one pass was done, as shown in Fig 1(e). Laser-A condition was initially adopted in order to produce a fast joining with only one pass. However, due to laser power limitation, it was necessary to perform two passes to obtain total penetration. The heat input for the laser-A condition was 40 J/mm for each pass and for the laser-B was 250 J/mm. As a result of the high welding speed, this condition of low heat input resulted in a thin weld bead, as seen in Fig 1(c). On the other hand, Laser-B condition was adopted in order to obtain total penetration with only one pass, as seen in Fig. 1(e). To do so, a low welding speed was necessary, and, consequently, a higher heat input. As seen in Fig. 1(c) and 1(d), small pores were found in Laser-A weld, mainly in the root, since there was no root protection by inert gas. It was also observed that, in some regions, the absence of total penetration, as shown in Fig. 1(d).

Table 1. Chemical composition of B550 steel

Designation	Chemical Composition (wt. pct.)							
	C	Mn	P	Si	S	Cr	Al	Others(1)
B 550	0.085	1.169	0.017	0.053	0.005	0.013	0.026	0.045

(1) Ni, V, Ti, Mo, Cu, Sn, B and N

ISSN 2176-5480

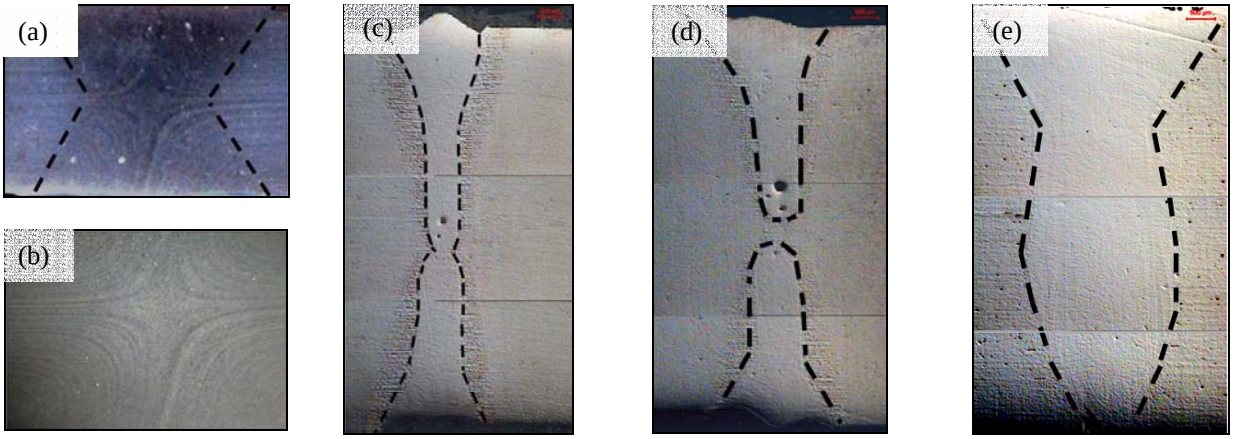

Figure 1 – Weld profiles as obtained by: (a) Flash welding with 1× magnification and (b) 5× magnification; (c) and (d) Laser-A with 50× magnification and (e) Laser-B with 50× magnification.

2.2 Specimens and experimental method

The tensile and fatigue crack growth (FCG) specimens were produced in accordance to the specifications of ASTM E8 and ASTM E647 standards, respectively, and the tests were conducted in a MTS servo-hydraulic system in laboratory air at room temperature. Four tensile tests were performed for each weld condition. The tensile testpieces were cut transversal to the weld, in such a way that the weld bead was centered in relation to the gage length, which, of course, also contained the Heat Affected Zone (HAZ) and base metal in its extremities. For the FCG tests, a Compact Tension C(T) testpiece was adopted, with the crack propagation line along the weld metal, HAZ (only for the flash-weld condition) and base metal. The crack line was induced by a pair of side grooves cut on the testpiece faces. The fatigue tests were conducted under constant amplitude loading, with sinusoidal waveform, frequency of 10 Hz and load ratio R = 0.1. Two FCG tests were performed for each condition. For the microstructural analysis, the samples were etched with Nital 10%. The micrographs were obtained via optical microscopy. The Vickers hardness profile, obtained by micro-indentation, followed ASTM E92 standard, with a load of 200 gf during 30 s. The fratographic analysis was performed via scanning electron microscopy (SEM). For comparison reasons, some results referring to SAE 1010 steel, traditionally employed by wheel makers, are also presented in this work.

3 RESULTS AND DUSCUSSION

3.1 Microstructural changes and microhardness profile

The microstructures of B550 and SAE 1010 steels are shown in Fig. 2(a) and (b), respectively. It can be seen that B550 steel, submitted to controlled rolling, presents equiaxial refined ferrite grains, elongated perlite colonies and some retained austenite, which is found mainly in the grain contours, that are remainder of regions rich in alloy elements that act as austenite stabilizers, such as Mn, Ni, Cu and C. The microstructure of SAE 1010 steel shows ferrite grains and small perlite colonies. It is evident the smaller grains size of B550 steel in comparison with SAE 1010 steel, another consequence of the controlled rolling to which the former is submitted.

The microstructures of the flash welded and laser beam welded regions are shown in Fig. 3(a), 3(b), 3(c) and 3(d). It can be seen the difference between the flash weld beads in SAE 1010, Fig. 3(a) and B550 steel, Fig. 3(b), with respect to the microstructural dimension, which is more refined in B550 steel. The phases and micro-constituents present in the weld beads are mostly similar (primary ferrite, grain-boundary ferrite, acicular ferrite and perlite), the only differences being the presence of Widmanstätten ferrite and retained austenite in B550 steel.

The analysis of the influence of the welding process/parameters on the microstructure of B550 steel (and, consequently, over its mechanical properties), can be initially done by comparison of Fig. 3(b), 3(c) and 3(d). Since the base metal is the same, and both processes are performed without metal addition, the microstructures of the weld beads are a result of the characteristics of each process and its parameters, and these are affected mainly by the heat input and cooling rate. The latter is influenced by the heat input itself, joint geometry and base metal. Because in this analysis the base metal and joint geometry are the same, only the heat input was taken in account. The heat input of the laser process is one order of magnitude lower than those found in the electric arc processes, as flash welding, and it is affected by three distinct factors: absorption, welding speed and laser power (Pekkarinen and Kujanpää, 2010). In this work, the laser power is not altered and the absorption effect can be disregarded, since it depends on the laser beam wave length and on the material to be welded (Quintino et al., 2007), both kept constant. The laser speed strongly affects the heat

ISSN 2176-5480

input: the higher the speed, the lower the heat amount generated in a weld bead section, resulting in high cooling rates that can lead to microstructural changes of the weld metal.

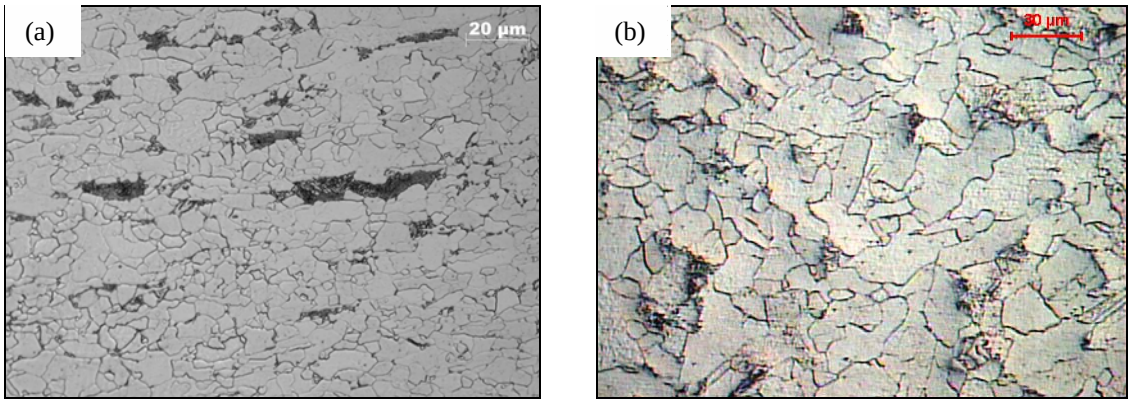

Figure 2 – Base metal microstructure, 500× magnification: (a) B550 steel, (b) SAE 1010 steel (etchant: Nital 10%).

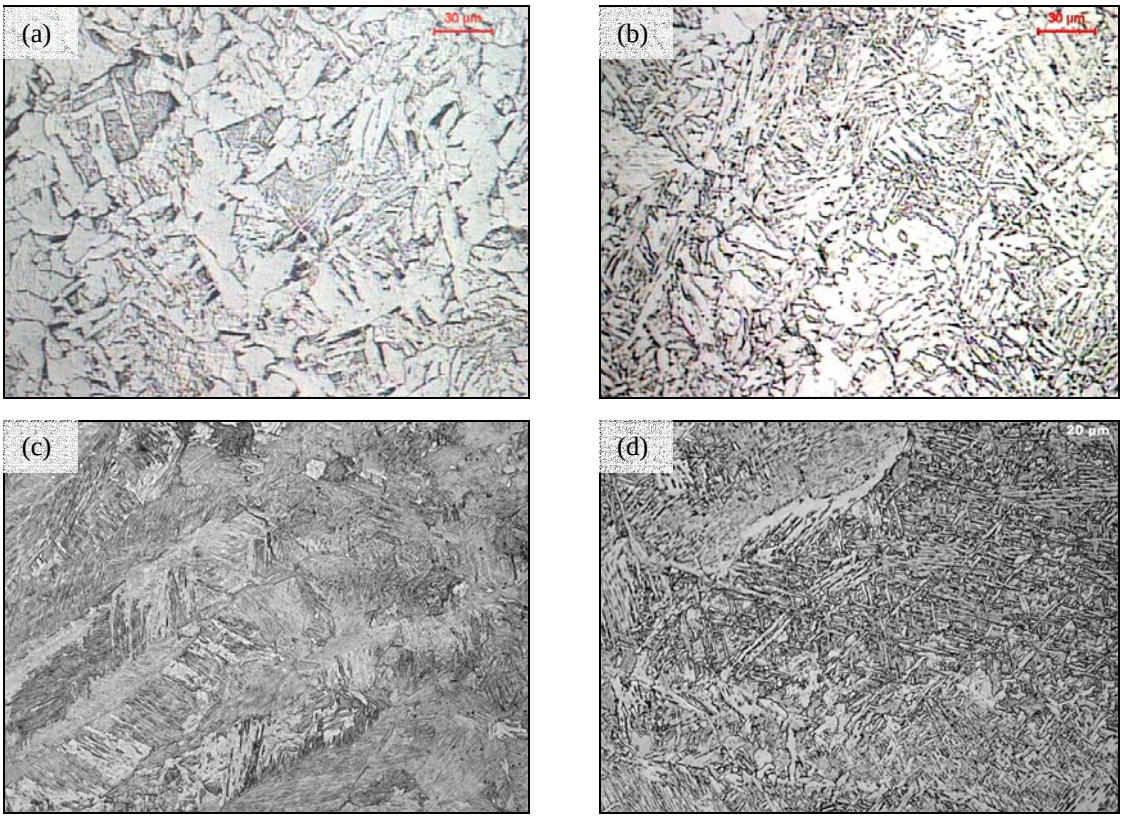

Figure 3 – Welded region microstructures, 500× magnification: (a) Flash-welded SAE 1010 steel, (b) Flash-welded B550 steel, (c) Laser welded (Laser-A) B550 steel, (d) Laser welded (Laser-B) B550 steel (etchant: Nital 10%).

The low heat input promoted by the laser welding process, as well as the heat dissipation of the steels, help the rapid cooling of the melting pool, leading to a microstructural refinement of the weld metal. The low nucleation energy for new phases offers more nucleation sites at low temperature, mainly in the austenite grain boundaries, favoring a huge grain nucleation and therefore a lower final grain size in the microstructure. The low temperature also favors the formation of Widmanstätten ferrite, acicular ferrite, martensite and bainite. Both tendencies, not observed in the flash welded joint, see Fig. 3(b) were found in the laser welds: grain refinement and the formation of a martensite and bainite-rich microstructure (Laser-A), see Fig. 3(c), and the formation of Widmanstätten and acicular ferrite (Laser-B), see Fig. 3(d). The flash welding process, as previously said, has a higher heat input, resulting in a coarse microstructure, mainly composed by primary ferrite, grain boundary ferrite, acicular ferrite and Widmanstätten ferrite.

ISSN 2176-5480

Similar results were found in other papers. Miranda et al. (2009) studied the API X100 HSLA steel welded by fibre laser beam and by the Tungsten Inert Gas (TIG) processes, both under two distinct heat inputs. The microstructure of the welded region was more refined when laser process was employed, resulting in better mechanical properties. The micro-constituents formed when the lower heat input was adopted were mainly martensite and bainite, and the higher heat input resulted in a coarser microstructure formed mainly by Widmanstätten ferrite. Jiamingo et al. (2010) evaluated the microstructure of a microalloyed steel after laser welding with low heat input and also found a microstructure rich in martensite and bainite.

The influence of the microstructure on the mechanical properties of the weld beads obtained in this work can be initially assessed by comparing the hardness profiles shown in Fig. 4.

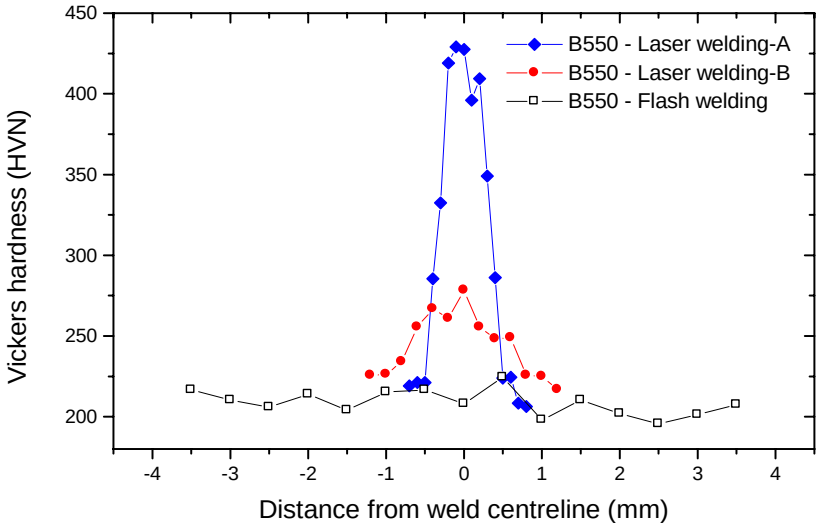

Figure 4 – Vickers hardness profiles.

The differences between the three welding conditions are evident from Fig. 4. As expected, the weld bead of B550 steel produced by condition Laser-A presented higher hardness (average value 415 HV), due to the presence of bainite and martensite in its microstructurem, see Fig. 3(c). The Laser-B weld region presented an average hardness of 260 HV, related to the refined microstructure, rich in acicular ferrite. Finally, the flash welding process resulted in a weld bead presenting an average hardness number of 200 HV. For the three conditions, the found hardness numbers are higher than the hardness of the base metal, 190 HV. For comparison, the average hardness of SAE 1010 steel is 145 HV and the flash welded region of this steel presented a hardness number of 165 HV. These values are in accordance to the fact that SAE 1010 steel has no addition of alloying elements and present a coarser microstructure than B550 steel.

Because the hardness measurements were performed at equidistant points, one can be infer from Fig. 4 about the differences between the sizes of the weld beads. The thin weld obtained by the laser process is evident, with an even smaller HAZ. The approximate sizes are 0.6 mm for Laser-A and 1.4 mm for Laser-B. On the other hand, the flash welding process resulted in welded regions as wide as 7 mm.

3.2 Tensile tests and fatigue crack growth behavior

For all of the welding conditions, the tensile testpieces fractured in the base metal region, which indicates that the joints were properly produced and all of the weld beads, as well as the corresponding HAZ, in spite of some existing discontinuities, have tensile strength higher than the base metal. In other words, the tensile tests for all of the welding conditions reflected the properties of the base metal, which are: σ_{ys} =459 MPa, σ_u =541 MPa and ΔL =32%.

The results of the FCG tests referring to crack propagation along the weld beads are shown in Fig. 5, and a comparison between the crack growth rates in base metal, HAZ and weld metal for flash-welded B550 steel in shown in Fig. 6. FCG tests with the crack propagating along the HAZ were performed only for flash welded samples, since the very small HAZ size obtained by the laser process make it unviable to grow a crack into this zone. The obtained FCG data correspond to stable regime (Region II of a FCG curve, also called the “Paris regime”), for which the crack propagation rate (*da/dN*) is approximately proportional to the variation of the stress intensity factor (ΔK) in a log-log plot, as seen in Fig. 5 and Fig. 6.

With respect to the FCG rate in the weld beads, shown in Fig. 5, small difference is observed between the adopted welding conditions in B550 steel. Moreover, it can be seen that, in comparison to flash welded SAE 1010 steel, all of the B550 joints show higher FCG resistance. For example, at a stress intensity factor range (ΔK) of de order of 25 MPa $m^{1/2}$, the FCG rate found in flash welded SAE 1010 steel is about $1x10^{-7}$ m/cycle, whereas for the flash welded B550 steel it is around 3.4 $x10^{-8}$ m/cycle. At the same ΔK, Laser-A joint presented 2.8 $x10^{-8}$ m/cycle and Laser-B, 5.6

ISSN 2176-5480

x10^{-8} m/cycle. This tendency of FCG resistance of the flash welded joint to be between the FCG resistances of the two laser joints prevails in the entire dataset.

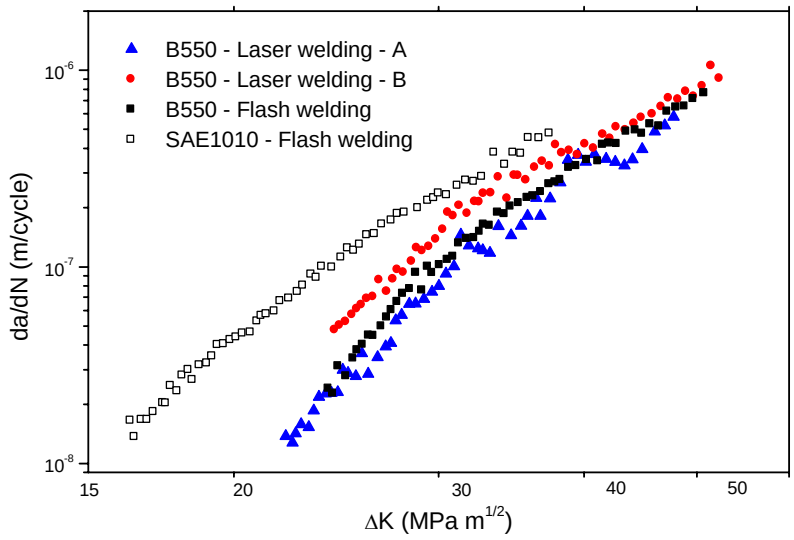

Figure 5 – FCG data (*da/dN* x *ΔK*) for crack propagating along weld metal, various welding conditions (*R* = 0.1).

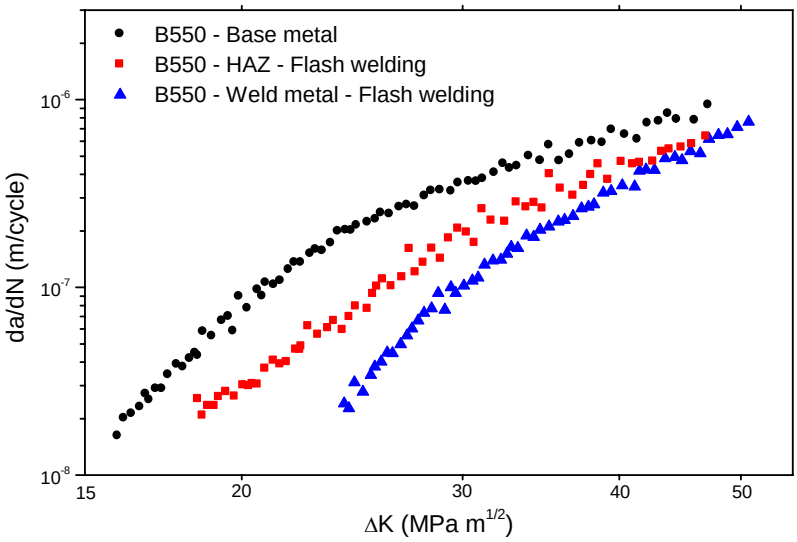

Figure 6 – FCG data (*da/dN* x *ΔK*) for flash welded B550 steel in three distinct regions (*R* = 0.1).

The comparison of the FCG data for B550 steel referring to base metal, HAZ (flash welding process) and weld metal, shown in Fig. 6, shows, for ΔK = 25 MPa $m^{1/2}$, crack propagation rates of 2.3 x10^{-7} m/cycle, 8.8 x10^{-8} m/cycle and 3.2 x10^{-8} m/cycle, respectively. The lowest FCG rate, found in the weld metal, is due to its refined microstructure, with high aspect ratio, which make the crack path more tortuous. The microstructure at the HAZ, detailed by Ribeiro et al. (2010) comprises ferritic grains smaller than those of base metal, as a result of the recrystallization that occurs in this region due to a combination of high temperature and plastic deformation promoted at the final stages of flash welding process. Comparison of both Figures 5 and 6 allows concluding that, no matter the welding process, the FCG resistance is always higher than the base metal.

Considering that the FCG tests were carried out under the same loading conditions and joint geometry, the differences in FCG rates can be evaluated in terms of the microstructure, joint properties and possible defects (flaws) produced during welding. The hardness results presented in Fig. 4 show elevated hardness number for Laser-A process when compared to the other conditions, although the difference in FCG rates was much less significant. Specifically among the tested weld beads, the best FCG resistance refers to that presenting the more refined microstructure (i.e. Laser-A condition). Similar results were obtained by other researchers: Balasubramanian et al. (2011) evaluated the mechanical behavior of welded joints in a titanium alloy, obtained by the following processes: Gas Tungsten Arc (GTAW), Electron Beam (EBW) and Laser Beam (LBW). They concluded that the weld bead microstructure was the reason for differences in the FCG rates presented by the joints. The higher FCG rates were presented by the GTAW joint, followed by EBW and LBW. The weld metal microstructure, in turn, was influenced by the heat input of the

ISSN 2176-5480

welding processes: the higher the heat input, slower the cooling rate and coarser the microstructure. The results of Miranda et al. (2009) for API X100 HSLA steel also confirm the effects of heat input: for 160 J/mm the microstructure of the weld bead was rich in martensite and bainite, and for 960 J/mm they obtained a ferritic microstructure. Jiaming Ni et al. (2010) evaluated laser welded joints in a microalloyed steel and observed that the joints presented a good combination of tensile strength and toughness, with values better than the base metal, and concluded that the refined microstructure of the weld bead, formed by bainite, interfered in crack propagation and was the main reason for the observed behavior. Tsay et al. (1996) obtained FCG data for a D6AC laser welded steel after various post-weld heat treatments. They encountered a condition for minimum FCG rate in comparison to base metal, and also attributed the obtained performance to the refined microstructure of weld metal and HAZ, formed mainly of bainite and tempered martensite.

As already mentioned, the microstructure (and consequently the related mechanical properties) has a strong influence on FCG rate, but other factors may be involved, such as the weld bead discontinuities or residual stresses. These factors possibly affected the results presented in this work, since it was expected that Laser-B condition (refined microstructure) would show higher FCG resistance in comparison to flash welded joint (coarse microstructure) in B550 steel. The explanation for this result may be related to the high amount of acicular ferrite found in the microstructure of Laser-B weld, see Fig. 3(d). According to Farrar and Harrinson (1987) this microstructural morphology tends to improve the mechanical properties of the weld bead, but, in large amounts (higher than 85% in volume) may impair the joint toughness. Another explanation may be related to possible discontinuities formed during the laser beam welding. It is known that pores and other discontinuities may increase the crack propagation rate, although it is necessary a huge amount of them (and larger sizes) to make this effect significant (Onõro and Ranninger, 1997). Finally, the observed result may also be related to residual stresses, that always are present in welded joints, and whose effect may be harmful or beneficial, depending on the stress in the analyzed site to be tensile or compressive (Jang et al., 2010).

3.3 Fracture Analysis

The fracture surfaces of the FCG testpieces were observed in a scanning electron microscope (SEM), operating in the secondary electrons mode. Figure 7 shows the fracture surfaces of base metal, HAZ and weld metal for flash welded B550 steel, corresponding to the beginning and to the final portion of stable crack propagation (Paris regime). These are shown, respectively, with 1,000× magnification, see Fig. 7(a), 7(b) and 7(c), and 5,000× magnification, Fig. 7(d), 7(e) and 7(f). Figures 8(a), 8(b) and 8(c) show the fracture surfaces at stable FCG regime, with 5,000× magnification, of B550 steel weld beads produced by flash welding, Laser-A and Laser-B processes, respectively.

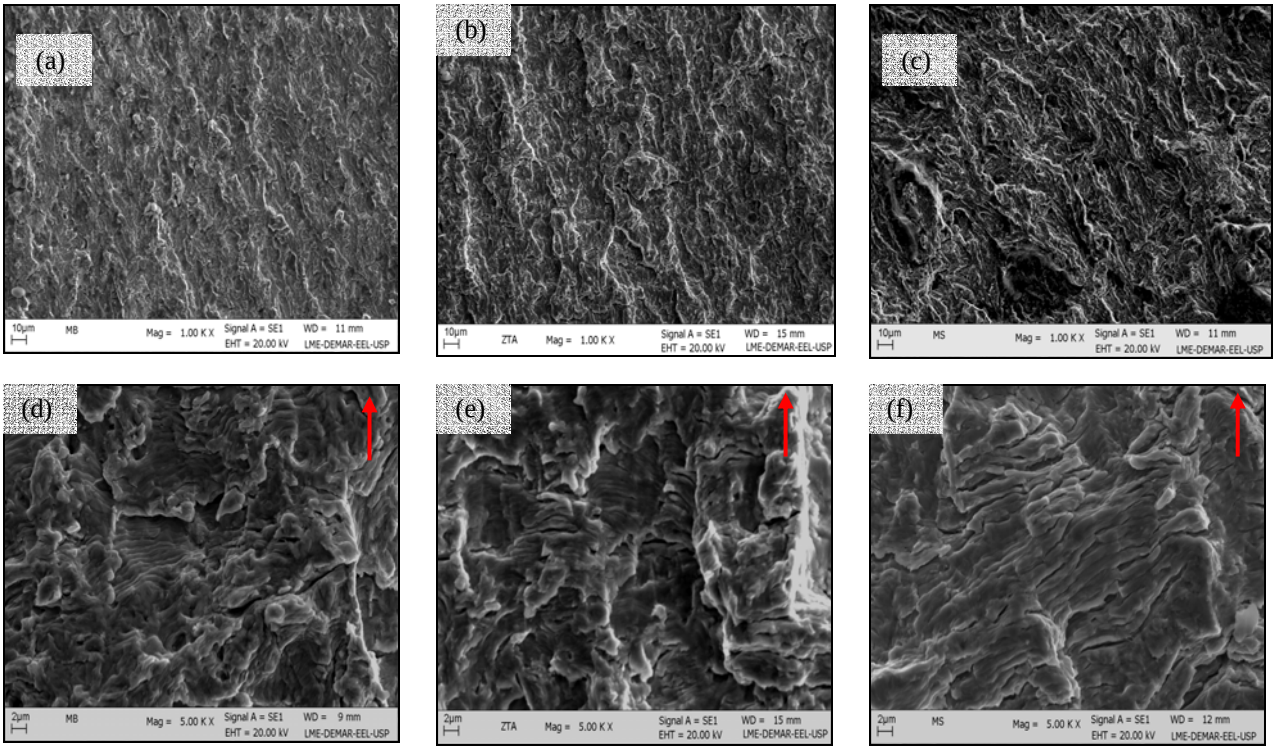

Figure 7 - Representative SEM fractographs steel B550: Start of propagation with 1000X magnification (a) Base metal; (b) Heat affected zone; (c) weld metal; and terminal of propagation with 5000X magnification (d) Base metal; (e) Heat affected zone; (f) weld metal.

It can be observed in Fig. 7 that the base metal region, Fig 7(a) present a greater number of deformation marks, due to its higher ductility, although these marks are less intense due to the simpler and more homogeneous microstructure. Secondary cracks are also seen. The HAZ, Fig. 7(b), in accordance to its intermediate properties, also show in its fracture intermediate characteristics between the two other regions. The weld metal fracture, Fig. 7(c), shows less deformation marks, indicating its lower deformation capacity, however these marks are more intense, because the microstructure is more complex and heterogeneous. A greater number of secondary cracks is also seen in this region. At the final portion of the stable regime, Fig. 7(d), 7(e) and 7(f), widespread deformation is observed in all conditions. The direction of crack propagation is indicated in the picture, and broad fatigue striations are also seen.

In Fig. 8, fatigue striations can be observed in the fracture surfaces of B550 weld metal of the three conditions: flash welded, Fig 8(a), Laser-A, Fig. 8(b), and Laser-B, Fig. 8(c). Fatigue striations can be seen in all of them. Although rigorous striation spacing measurements were not done, it can be observed that striation spacing is much smaller in Laser-A fracture surface, indicating a lower crack propagation rate for this condition and, consequently, its tendency to show a better FCG resistance.

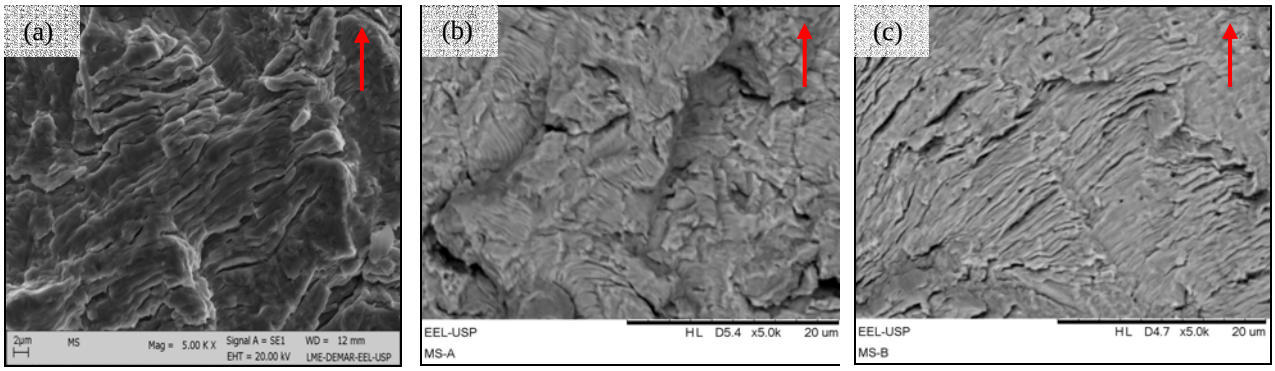

Figure 8 – Representative SEM fractographs, B550 steel weld metal: (a) Flash welding; (b) Laser-A; (c) Laser-B (magnification: 5,000×).

4. CONCLUSIONS

The characterization of welded joints in B550 steel, obtained by flash welding and laser beam welding processes, and the comparison with flash welded SAE1010 steel joints, by means of microsctructural analysis, tensile tests, Vickers hardnes measurements and fatigue crack growth tests led to the following conclusions:

- good quality joints were produced by both processes with the adopted parameters and, although some small discontinuities such as pores were found in the weld beads, the mechanical properties of the joints were better than those of the base metal.
- The microstructure and mechanical properties of the weld metal are influenced by the process and welding parameters. The heat input is a major factor affecting the final characteristics of the joint.
- For HSLA B550 steel, the lower heat input associated to the process named Laser-A resulted in a martensite and bainite-rich microstructure, presenting higher hardness and fatigue crack growth resistance.
- Laser-B process, having higher heat input than Laser-A and in which the joint is produced in only one pass, resulted in acicular ferrite presenting intermediate hardness number and crack propagation rates.
- Flash welding process, having the highest heat input among the studied processes, resulted in a coarse microstructure, in which various ferrite morphologies coexist, and presenting the lowest hardness and fatigue crack growth resistance.
- All of the B550 joints presented better mechanical properties than the conventional SAE 1010 flash welded joint, indicating that the material replacement is viable on the point of view of the material and welding process.

5. ACKNOWLEDGEMENTS

The authors are thankful to IOCHPE-MAXION (Cruzeiro/SP).

6. REFERENCES

Balasubramanian, T.S., Balasubramanian, V., Muthu Manickam, M.A., 2011. “Fatigue crack growth behaviour of gas tungsten arc, electron beam and laser beam welded Ti-6Al-4V alloy”. In *Materials and Design* 32, 4509-4520.

Chung, B. G., Rhee, S., Lee, C. H., 1999. “The effect of shielding gas type on CO_2 laser tailores blank weldability of low carbon automotive galvanized steel”. In *Materials Science and Engineering* A272: 357-362.

ISSN 2176-5480

Fabari, N., Chen, D.L., Li, J., Zhou, Y., Dong., 2010. “Microstruture and mechanical properties of laser welded DP600 steel joints”. In *Materials Science and Engineering A* 527, 1215-1222.

Farrar, A., Harrinson P. L., 1987.“Acicular Ferrite in Carbon-Manganese Weld Metals”. In *Journal of Materials Science* 22, 3812-3820.

Ichiyama, Y., Kodama, S., 2007. “Flash-Butt Welding of High Strength Steels”. In *Nippon Steel Technical Report* 95.

Jang, C., Cho, P.Y., Kim, M., Oh, S.J., Yang, J.S., 2010. “Effects of microstructure and residual stress on fatigue crack growth of stainless steel narrow gap welds”. In *Materials and Desing*, v.31, p. 1862-1870.

Jiaming Ni., Zhuguo Li., Huang, J., Wu, Y., 2010.“Strengthening behavior analysis of metal of laser hybrid wlding for microalloyed stell”. In *Materials and Design* 31, 4876-4880.

Kang, S. S., Min, K. B., 2000. “A study on resistance welding in steel sheets for tailor welded blank Evaluation of Flash weldability and formability”. In *J. of Mater Process*, Technol, 103: 218-224.

Lin Li., Eghlio, R., Marimuthu, S., 2011. “Laser net shape welding”. In *Manufacturing technology* 60, 223-226.

Mei, L., Chen, Genyu., Jin, X., Zhang, Y., Wu, Q., 2009. “Research on laser welding of high-strength galvanized automobile steel sheets”. In *Optics and Lasers in Enginnering* 47: 1117-1124.

Miranda, R., Costa, A., Quintino, L., Yapp, D., Iordachescu, D. 2009. “Caracterization of fiber laser welds in X100 pipeline steel”. In *Materials and Desing* 30, 2701-2707.

Onõro, J., Ranninger, C., 1997. “Fatigue behavior of laser welds of high-strength low-alloy steels”. In *Journal of Materials Processing Techology* 68, 68-70.

Pekkarinen, J., Kujanpää, V., 2010. “The effects of laser welding parameters on the microstruture of ferritic and duplex stainless steels welds”. In *Physics Procedia* 5, 517-523.

Quintino, L., Costa, A., Miranda, R., Yapp, D., Kumar, V., Kong, C.J., 2007. “Welding with high power fiber lasers – A preliminary study”. In *Materials and Design* 28, 1231-1237.

Ribeiro, H. V., Versuto B. C. B., Baptista, C. A. R. P., 2010. “Microstructural and mechanical characterization of flash-welded joints in HSLA steels”. In *SAE Technical Paper Series*, v. 1, p. 1-5.

Saito, T., Ichiyama, Y., 1996. “Weld defects and evaluation of weld quality: Welding phenomena and process control in flash welfing of steel sheets”. In *Welding International 10 (2), 117-123.*

Tsay, L. W., Chung, C.S., Chent, C., 1996. “Fatigue crack propagation of D6AC laser welds”. In *Int. J. Fatigue* Vol.19, 0025-31.

Yi, Z., Genyu, C., Lijun Li., 2008. “3D heat transfer in laser deep penetration welding based on real keyhole”. In *Chinese Journal of Lasers* 29(2):27–30.

7. RESPONSIBILITY NOTICE

The authors are the only responsible for the printed material included in this paper.